CHEMISTRY OF MATERIALS
Cite This: Chem. Mater. 2018, 30, 1825−1829
Communication
pubs.acs.org/cm

$NaFeF_3$ Nanoplates as Low-Cost Sodium and Lithium Cathode Materials for Stationary Energy Storage

Kostiantyn V. Kravchyk,[†,‡] Tanja Zünd,[†,‡] Michael Wörle,[†] Maksym V. Kovalenko,*[,†,‡] and Maryna I. Bodnarchuk*[,‡]

[†]Laboratory of Inorganic Chemistry, Department of Chemistry and Applied Biosciences, ETH Zürich, Vladimir-Prelog-Weg 1, CH-8093 Zürich, Switzerland

[‡]Laboratory for Thin Films and Photovoltaics, Empa − Swiss Federal Laboratories for Materials Science and Technology, Überlandstrasse 129, CH-8600 Dübendorf, Switzerland

Supporting Information

Phasing out fossil fuels and replacing them with CO_2-emission-free renewables, such as solar and wind, remains a great challenge, as it requires the integration of large and inexpensive stationary rechargeable batteries into the electric grid to stabilize the energy production−consumption mismatch caused by the intermittent nature of these energy sources.[1,2] The energy density of these stationary batteries is of secondary significance in comparison to the cost of stored energy per cycle (expressed in ¢/kWh-cycle). Stringent cost requirements for grid-scale batteries can be met only with low-cost and easy-to-produce battery components. To achieve this goal, lithium and sodium rechargeable battery technologies based on inexpensive cathode materials composed of highly abundant elements are being intensely explored.[3−6] In this context, batteries that employ a $NaFeF_3$ fluoroperovskite cathode present numerous advantages, such as earth abundance of its chemical elements, its intrinsically high oxidative stability, and its high theoretical capacity of 197 mAh g^{-1} for one-electron operation.[7−12] Upon electrochemical charging in sodium or lithium electrolytes, Na ions can be deintercalated from the $NaFeF_3$ structure, forming a FeF_3 phase with concomitant sodiation/lithiation of the anode (Figure 1). The fundamentally important advantage is that a $NaFeF_3$ cathode can be paired with sodium/lithium-free anodes (e.g., graphite, hard carbon, Si). However, alkali-metal-free iron fluorides cannot be used for the full-cell configuration, unless they are paired with exotic Li/Na-containing anodes. Furthermore, $LiFeF_3$ remains elusive; i.e., it has never been synthesized and it is predicted to be thermodynamically unstable, making $NaFeF_3$ essentially the only choice for Li ion storage.[8]

$NaFeF_3$, nevertheless, still faces a number of obstacles before it can be practically deployed. The foremost issue is its high electrical resistance, which is caused by the ionic characteristics of the metal−fluoride bond. At best, this limits the cyclability of the battery, especially under high C-rates.[7,9−11] At worst, it drastically reduces the achievable capacity. However, this problem can be partially resolved both by downsizing the bulk material to the nanoscale and by mixing it with conductive additives, such as amorphous carbon particles. This allows for percolation, which enables electronic transport in the electrode, and a short conduction path within the insulating phase.[13] As an example, highly electronically insulating $LiFePO_4$ became a practical cathode material and was eventually commercialized only after its mean primary crystallite size was reduced to below 100 nm.[14] Therefore, it is highly desirable to solve the inherent issue of the $NaFeF_3$ cathode's low electronic conductivity via direct nanoscale synthesis to pave a path for its application as a cost-effective cathode for stationary energy storage.

We chose sodium−iron hexafluoroacetylacetone $NaFe(hfac)_3$ as a precursor for the colloidal synthesis of $NaFeF_3$ NPLs. Inexpensive synthesis of this compound was recently reported by Dikarev et al.[15] The chemical bonding in crystalline $NaFe(hfac)_3$ is depicted in Figure 2.[15] $NaFe(hfac)_3$ is synthesized in a high yield using a one-step reaction between

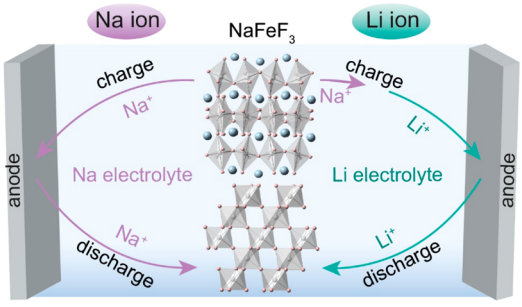

Figure 1. Schematics of the charge and discharge process of the $NaFeF_3$ cathode and sodium/lithium-free anodes in a full-cell configuration with sodium and lithium electrolytes.

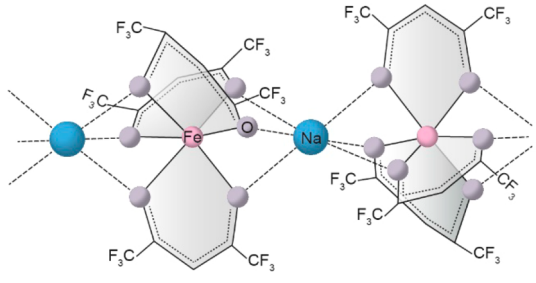

Figure 2. Fragment of the chemical structure of crystalline $NaFe(hfac)_3$.

Received: November 10, 2017
Revised: March 10, 2018
Published: March 12, 2018

DOI: 10.1021/acs.chemmater.7b04743
Chem. Mater. 2018, 30, 1825−1829

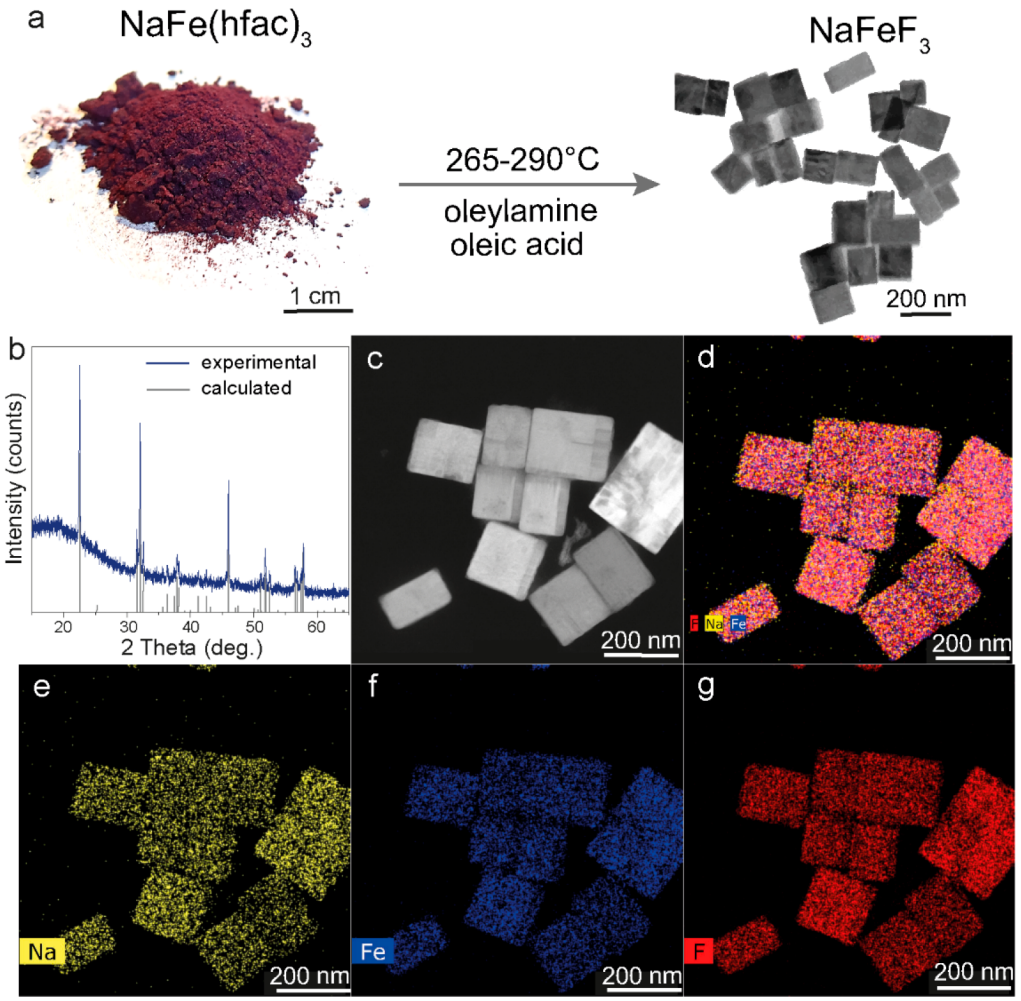

Figure 3. (a) Schematics of the one-pot synthesis of $NaFeF_3$ NPLs; (b) powder X-ray diffraction pattern and (c) HAADF-STEM image of $NaFeF_3$ NPLs; (d) composite of the color maps shown in (e), (f), and (g); (e) Na Kα, (f) Fe Kα, and (g) F Kα color maps extracted from a EDS-STEM hypermap acquired from $NaFeF_3$ NPLs.

sodium hexafluoroacetylacetone and iron(II) chloride in acetone. We note that the only work that has been previously reported on the electrochemical performance of sodium metal fluoride nanocrystals was performed by Yamaki et al.[10,16] Nanosized (10−600 nm) $NaFeF_3$ was produced using a liquid phase synthesis in a mixture of oleic acid and oleylamine by reacting iron and sodium trifluoroacetates. The $NaFeF_3$ NCs exhibited discharge capacities ranging from 181 to 45 mA h g^{-1} for sodium ion storage when the current rate was varied from 0.01 to 1 C. These results showed that nanoscopic $NaFeF_3$ is capable of operation at close to its theoretical charge-storage capacity, unlike the bulk material.

Here, we report a simple synthetic route for crystalline $NaFeF_3$ NPLs through the thermal decomposition of heterometallic, fluorinated, β-diketonate $NaFe(hfac)_3$ in benzyl ether or 1-octadecene (ODE) with oleic acid (OAc) and oleylamine (OAm) as ligands. We determined that the $NaFeF_3$ NPLs exhibit a high cyclic stability as cathode materials in both sodium and lithium ion batteries, delivering initial capacities of 153 mAh g^{-1} and 183 mAh g^{-1}, respectively. Half of these capacities were retained after prolonged operation over 200 cycles at a current density of 0.2 A g^{-1} (~1 C).

Figure 3a outlines the liquid-phase synthesis of high-quality $NaFeF_3$ NPLs using $NaFe(hfac)_3$ as a single-source precursor, benzyl ether, or 1-octadecene as high boiling point organic solvents and OAc and OAm as the surface capping ligands. The combination of solvents and various possible ligands is essential for the preparation of phase-pure and monodispersed $NaFeF_3$ NPLs. Decomposition of $NaFe(hfac)_3$ in pure ODE or benzyl ether in the absence of ligands leads to the oxidation of Fe(II) to Fe(III). The final product contains either bulk Na_3FeF_6 or a mixture of Na_3FeF_6 and $NaFeF_3$ fluorides. We further assume that OAm might serve as a mild reducing agent that prevents the oxidation to Fe(III). To obtain monodisperse, pure-phase NPLs, an appropriate combination of solvents and OAc/OAm is necessary in the synthesis. The thermal decomposition of (hfac)-compounds might follow a process similar to that seen in better-studied trifluoroacetates.[16−22] For the latter cases, it is assumed that, after decarboxylation, a CF_3^- anion is formed, which subsequently dissociates into a fluoride ion (F^-) and difluorocarbene (CF_2).[23] F^- is then combined with a metal ion to form the corresponding metal fluoride. Uniform, square-shaped 100 nm NPLs of $NaFeF_3$ were produced when the 0.5 mmol precursor was combined with the OAc/OAm mixture (1:1 volume ratio) and heated at 260 °C for 60 min. Representative transmission electron microscopy (TEM) and scanning transmission electron microscopy (STEM) images of the $NaFeF_3$ NPLs are shown in Figure S1a−c, respectively. The

DOI: 10.1021/acs.chemmater.7b04743
Chem. Mater. 2018, 30, 1825−1829

STEM images are acquired with the atomic number sensitive, high-angle annular dark field detector (HAADF STEM). When a larger amount of OAc was added to the reaction mixture (OAc/OAm = 2:1), the final product again contained a mixture of Na_3FeF_6/$NaFeF_3$ fluorides. Under the opposite conditions (OAc/OAm = 1:2), spherical Fe_3O_4 nanoparticles and a mixture of fluorides were obtained. Excessive OAm could lower the reactivity of F^- ions, inhibiting the formation of $NaFeF_3$ and promoting the formation of oxides (from the decomposition of Fe oleates).[16] When other ligands, such as trioctylphosphine, were introduced, iron(II) fluoride appeared as a side product. Temperature was another important factor. Short reaction times and temperatures below 240 °C often yielded NaF impurities, even at the optimized OA/OAm ratio of 1:1.

As illustrated in Figure 3b, the powder X-ray diffraction (XRD) pattern of pure-phase $NaFeF_3$ NPLs shows an orthorhombic perovskite structure with the space group *Pnma*. The orthorhombic lattice parameters, refined by Rietveld method, are a = 5.6651(4) Å, b = 7.8869(6) Å, and c = 5.4879(4) Å (Figure S2, Table S1). As follows from the high-resolution transmission electron microscopy (HRTEM) image (see Figure S3), the top facet of the $NaFeF_3$ NPLs is a plane (100).

The elemental distribution of Na, Fe, and F within the NPLs was examined by energy dispersive spectroscopy (EDS) employed in the STEM operation mode using about 0.7−0.8 nm probe size (Figure 3c−g). A certain amount of the oxygen signal (Figure S4a) can be attributed to the minor oxidation of the NPLs during the synthesis, cleaning, or the preparation procedure of the TEM specimen. X-ray lines for F Kα and Fe Lα are close in energy, with a difference of only 27 eV. As follows from the electron energy loss spectroscopy (EELS) spectra of $NaFeF_3$ NPLs (Figure S4b), the Fe-L_{23}-edge is represented by the L_3 and L_2 lines, whereas the other lines correspond to the K-edge of the fluorine.

The presence of this two-peak feature in the F−K-edge has been previously observed for other metal fluorides. The main peak of the F−K-edge, centered at 684 eV, is attributed to the covalently bonded fluorine, likely stemming from the possible C−F bonded organic side product.

Prior to the electrochemical experiments, highly insulating long-chain capping ligands (OA/Oam) had to be removed through mild chemical treatment. We found that the hydrazine-based ligand-removal protocol, which was initially developed for colloidal quantum dots,[24] was highly effective in rendering the $NaFeF_3$ NPLs organic-ligand-free (see Figure S5). Untreated, organic-capped $NaFeF_3$ NPLs yielded no operational electrodes.

For the electrochemical measurements, the $NaFeF_3$ electrodes were prepared by mixing a powder of $NaFeF_3$ NPLs with carbon black (CB), polyvinylidene fluoride (PVdF), and *N*-methylpyrrolidone (NMP), and the resulting slurries were cast onto an aluminum foil as a current collector. Coin-type cells were employed for the electrochemical tests. The cell consisted of a sodium or lithium disk as a counter and reference electrode and $NaFeF_3$ as a working electrode, and a glass−fiber separator was placed in between both electrodes and soaked with a sodium or lithium electrolyte. All electrochemical measurements were performed using the constant-current/constant-voltage (CCCV) method of charging within insertion region (between 1.5 and 4 V and 2−4.2 V for Na ion and Li ion cells, accordingly, see Figure S6).

Figure 4a shows the typical voltage profiles of the Na and Li ion half-cells employing $NaFeF_3$ NPLs as an active material at a

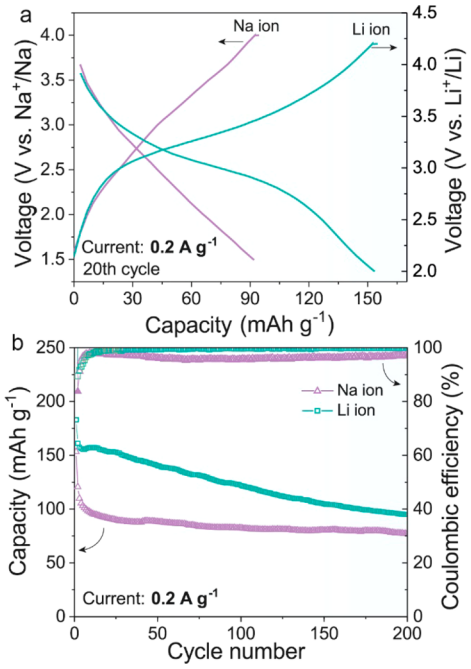

Figure 4. Electrochemical performance of $NaFeF_3$ NPLs cycled with sodium and lithium electrolytes in a half-cell configuration using metallic sodium and lithium as the counter and reference electrodes, respectively. (a) Galvanostatic charge−discharge curves during the 20th cycle at a current density of 0.2 A g^{-1}; (b) cyclic stability measured at a current density of 0.2 A g^{-1}.

relatively high current density of 0.2 A g^{-1}. After the 20th cycle, Na and Li ion storage capacities of 91 mAh g^{-1} and 155 mAh g^{-1} were obtained, respectively, indicating suitable electronic conductivity and charge-transfer kinetics in the $NaFeF_3$ cathodes. The shape of the voltage profiles as well as the cyclic voltammetry (CV) curves for Na ion storage (Figure S7a) were rather smooth, suggesting a slow and gradual desodiation of the $NaFeF_3$ NPLs, without the formation of intermediate phases, even at a very low current density of 20 mA g^{-1} (Figure S7b). In fact, such behavior with stretched-out features in the CV curves and voltage profiles is rather typical for nanostructured materials, as frequently reported in the past.[25] Galvanostatic voltage profiles of the $NaFeF_3$ NPLs in the Li ion experiments were characterized by pronounced plateaus at ca. 3.05 V for both charging and discharging.

When the $NaFeF_3$ NPLs are cycled in a lithium electrolyte, Na deintercalation occurs during the first cycle, and subsequent Li insertion occurs during the second charging. As follows from the CV curves (Figure S8), desodiation during the first charge was characterized by a broad anodic peak at 3.3−3.8 V vs Li^+/Li. Subsequent CV cycling was characterized by well-defined anodic and cathodic peaks at 3.24 V and 2.8−3.1 V vs Li^+/Li.

The cycling stability tests of half-cells employing $NaFeF_3$ NPLs at a current density of 0.2 A g^{-1} showed a high capacity retention of 50% and 52% after 200 cycles for sodium and lithium ion storage, respectively (Figure 4b). These are among the longest-lasting fluoride-based cathodes reported to date (see Table S2 for a detailed comparison).[7−10,16,18,22,26−45] In fact, it is the first observation of stable cycling of this compound. The pioneer work of Yamaki et al.[10] on $NaFeF_3$

DOI: 10.1021/acs.chemmater.7b04743
Chem. Mater. 2018, 30, 1825−1829

NCs did not report cycling experiments. We note that $NaFeF_3$ NPLs showed poor cyclic performance using those voltage intervals, which includes both insertion and conversion regions, respectively (1.5−4.2 V vs Li^+/Li, see Figure S9).

In summary, we have reported a simple colloidal synthesis of highly uniform and highly crystalline $NaFeF_3$ NPLs by thermal decomposition of a single-source precursor, $NaFe(hfac)_3$, in high boiling point solvents and in the presence of long alkyl chain ligands. The solvent/ligands ratio was found to be a primary factor for obtaining phase-pure nanomaterials. After the removal of the insulating ligands, the electrochemical storage of Na and Li ions in the $NaFeF_3$ NPLs was assessed. The $NaFeF_3$ NPLs are capable of fast electrochemical extraction/insertion of sodium and lithium ions. In particular, high initial capacities of 153 mAh g^{-1} and 183 mAh g^{-1} were obtained at a current density of 0.2 A g^{-1} (~1C) for sodium and lithium ion storage, respectively. At least 50% of these capacities were retained after 200 cycles. This work overcomes the major constraint associated with the low electronic conductivity of $NaFeF_3$ and affirms that such perovskite-based metal fluorides are promising low-cost electrode materials for Li and Na ion batteries.

■ ASSOCIATED CONTENT

Supporting Information

The Supporting Information is available free of charge on the ACS Publications website at DOI: 10.1021/acs.chemmater.7b04743.

Materials and details of $NaFeF_3$ NCs synthesis and additional electrochemical, XRD, FTIR, and TEM data (PDF)

■ AUTHOR INFORMATION

Corresponding Authors

*(M.I.B.) E-mail: maryna.bodnarchuk@empa.ch.
*(M.V.K.) E-mail: mvkovalenko@ethz.ch.

ORCID

Maksym V. Kovalenko: 0000-0002-6396-8938

Author Contributions

All authors have given approval to the final version of the manuscript.

Notes

The authors declare no competing financial interest.

■ ACKNOWLEDGMENTS

This work was financially supported by the Swiss National Science Foundation (SNF Ambizione Energy grant, Grant No. PZENP2_154287), the Swiss Federal Commission for Technology and Innovation (CTI) through the Swiss Competence Centers for Energy Research (SCCER, "Heat and Electricity Storage"), and the Competence Center for Energy and Mobility (CCEM, Project SLIB). The authors thank Dr. Alla Sologubenko for EELS measurements and spectra analysis. The authors are grateful to the research facilities of ETH Zurich (ETH Electron Microscopy Center, Department of Chemistry and Applied Biosciences) and Empa (Empa Electron Microscopy Center) for access to the instruments and for technical assistance.

■ REFERENCES

(1) Van Noorden, R. A Better Battery. *Nature* **2014**, *507*, 26−28.
(2) Larcher, D.; Tarascon, J. M. Towards Greener and More Sustainable Batteries for Electrical Energy Storage. *Nat. Chem.* **2015**, *7*, 19−29.
(3) Wang, L.; Lu, Y.; Liu, J.; Xu, M.; Cheng, J.; Zhang, D.; Goodenough, J. B. A Superior Low-Cost Cathode for a Na-Ion Battery. *Angew. Chem., Int. Ed.* **2013**, *52*, 1964−1967.
(4) Palomares, V.; Serras, P.; Villaluenga, I.; Hueso, K. B.; Carretero-Gonzalez, J.; Rojo, T. Na-ion batteries, recent advances and present challenges to become low cost energy storage systems. *Energy Environ. Sci.* **2012**, *5*, 5884−5901.
(5) Qian, J.; Zhou, M.; Cao, Y.; Ai, X.; Yang, H. Nanosized $Na_4Fe(CN)_6$/C Composite as a Low-Cost and High-Rate Cathode Material for Sodium-Ion Batteries. *Adv. Energy Mater.* **2012**, *2*, 410−414.
(6) Liu, J.; Wan, Y.; Liu, W.; Ma, Z.; Ji, S.; Wang, J.; Zhou, Y.; Hodgson, P.; Li, Y. Mild and Cost-Effective Synthesis of Iron Fluoride-Graphene Nanocomposites for High-Rate Li-Ion Battery Cathodes. *J. Mater. Chem. A* **2013**, *1*, 1969−1975.
(7) Gocheva, I. D.; Nishijima, M.; Doi, T.; Okada, S.; Yamaki, J.-i.; Nishida, T. Mechanochemical Synthesis of $NaMF_3$ (M = Fe, Mn, Ni) and Their Electrochemical Properties as Positive Electrode Materials for Sodium Batteries. *J. Power Sources* **2009**, *187*, 247−252.
(8) Dimov, N.; Nishimura, A.; Chihara, K.; Kitajou, A.; Gocheva, I. D.; Okada, S. Transition Metal $NaMF_3$ Compounds as Model Systems for Studying the Feasibility of Ternary Li-M-F and Na-M-F Single Phases as Cathodes for Lithium−Ion and Sodium−Ion Batteries. *Electrochim. Acta* **2013**, *110*, 214−220.
(9) Kitajou, A.; Komatsu, H.; Chihara, K.; Gocheva, I. D.; Okada, S.; Yamaki, J.-i. Novel Synthesis and Electrochemical Properties of Perovskite-Type $NaFeF_3$ for a Sodium-Ion Battery. *J. Power Sources* **2012**, *198*, 389−392.
(10) Yamada, Y.; Doi, T.; Tanaka, I.; Okada, S.; Yamaki, J.-i. Liquid-phase Synthesis of Highly Dispersed $NaFeF_3$ Particles and Their Electrochemical Properties for Sodium-ion Batteries. *J. Power Sources* **2011**, *196*, 4837−4841.
(11) Nava-Avendaño, J.; Arroyo-de Dompablo, M. E.; Frontera, C.; Ayllón, J. A.; Palacín, M. R. Study of Sodium Manganese Fluorides as Positive Electrodes for Na-Ion Batteries. *Solid State Ionics* **2015**, *278*, 106−113.
(12) Yu, S.; Zhang, P.; Wu, S. Q.; Li, A. Y.; Zhu, Z. Z.; Yang, Y. Understanding the Structural and Electronic Properties of the Cathode Material $NaFeF_3$ in a Na-Ion Battery. *J. Solid State Electrochem.* **2014**, *18*, 2071−2075.
(13) Oszajca, M. F.; Bodnarchuk, M. I.; Kovalenko, M. V. Precisely Engineered Colloidal Nanoparticles and Nanocrystals for Li-Ion and Na-Ion Batteries: Model Systems or Practical Solutions? *Chem. Mater.* **2014**, *26*, 5422−5432.
(14) Julien, C. M.; Mauger, A.; Zaghib, K. Surface Effects on Electrochemical Properties of Nano-Sized $LiFePO_4$. *J. Mater. Chem.* **2011**, *21*, 9955−9968.
(15) Wei, Z.; Filatov, A. S.; Dikarev, E. V. Volatile Heterometallic Precursors for the Low-Temperature Synthesis of Prospective Sodium Ion Battery Cathode Materials. *J. Am. Chem. Soc.* **2013**, *135*, 12216−12219.
(16) Du, Y. P.; Zhang, Y. W.; Yan, Z. G.; Sun, L. D.; Gao, S.; Yan, C. H. Single-Crystalline and Near-Monodispersed $NaMF_3$ (M = Mn, Co, Ni, Mg) and $LiMAlF_6$ (M = Ca, Sr) Nanocrystals from Cothermolysis of Multiple Trifluoroacetates in Solution. *Chem. - Asian J.* **2007**, *2*, 965−974.
(17) Baillie, M. J.; Brown, D. H.; Moss, K. C.; Sharp, D. W. A. Anhydrous Metal Trifluoroacetates. *J. Chem. Soc. A* **1968**, *0*, 3110−3114.
(18) Oszajca, M. F.; Kravchyk, K. V.; Walter, M.; Krieg, F.; Bodnarchuk, M. I.; Kovalenko, M. V. Colloidal BiF_3 Nanocrystals: A Bottom-Up Approach to Conversion-Type Li-Ion Cathodes. *Nanoscale* **2015**, *7*, 16601−16605.
(19) Ye, X.; Collins, J. E.; Kang, Y.; Chen, J.; Chen, D. T.; Yodh, A. G.; Murray, C. B. Morphologically Controlled Synthesis of Colloidal

DOI: 10.1021/acs.chemmater.7b04743
Chem. Mater. 2018, 30, 1825−1829

Upconversion Nanophosphors and Their Shape-Directed Self-Assembly. *Proc. Natl. Acad. Sci. U. S. A.* **2010**, *107*, 22430−22435.
(20) Paik, T.; Ko, D. K.; Gordon, T. R.; Doan-Nguyen, V.; Murray, C. B. Studies of Liquid Crystalline Self-Assembly of GdF3 Nanoplates by In-Plane, Out-of-Plane SAXS. *ACS Nano* **2011**, *5*, 8322−8330.
(21) Boyer, J. C.; Vetrone, F.; Cuccia, L. A.; Capobianco, J. A. Synthesis of Colloidal Upconverting $NaYF_4$ Nanocrystals Doped with Er^{3+}, Yb^{3+} and Tm^{3+},Yb^{3+} via Thermal Decomposition of Lanthanide Trifluoroacetate Precursors. *J. Am. Chem. Soc.* **2006**, *128*, 7444−7445.
(22) Guntlin, C. P.; Zünd, T.; Kravchyk, K. V.; Wörle, M.; Bodnarchuk, M. I.; Kovalenko, M. V. Nanocrystalline FeF_3 and MF_2 (M = Fe, Co, and Mn) from Metal Trifluoroacetates and Their Li(Na)-Ion Storage Properties. *J. Mater. Chem. A* **2017**, *5*, 7383−7393.
(23) Blake, P. G.; Pritchard, H. The Thermal Decomposition of Trifluoroacetic Acid. *J. Chem. Soc. B* **1967**, *0*, 282−286.
(24) Talapin, D. V.; Murray, C. B. PbSe Nanocrystal Solids for n- and p-Channel Thin Film Field-Effect Transistors. *Science* **2005**, *310*, 86−89.
(25) Goriparti, S.; Miele, E.; De Angelis, F.; Di Fabrizio, E.; Proietti Zaccaria, R.; Capiglia, C. Review on Recent Progress of Nanostructured Anode Materials for Li-Ion Batteries. *J. Power Sources* **2014**, *257*, 421−443.
(26) Arai, H.; Okada, S.; Sakurai, Y.; Yamaki, J.-i. Cathode Performance and Voltage Estimation of Metal Trihalides. *J. Power Sources* **1997**, *68*, 716−719.
(27) Badway, F.; Cosandey, F.; Pereira, N.; Amatucci, G. G. Carbon Metal Fluoride Nanocomposites: High-Capacity Reversible Metal Fluoride Conversion Materials as Rechargeable Positive Electrodes for Li Batteries. *J. Electrochem. Soc.* **2003**, *150*, A1318−A1327.
(28) Nishijima, M.; Gocheva, I. D.; Okada, S.; Doi, T.; Yamaki, J.-i.; Nishida, T. Cathode Properties of Metal Trifluorides in Li and Na Secondary Batteries. *J. Power Sources* **2009**, *190*, 558−562.
(29) Bai, Y.; Zhou, X.; Zhan, C.; Ma, L.; Yuan, Y.; Wu, C.; Chen, M.; Chen, G.; Ni, Q.; Wu, F.; et al. 3D Hierarchical Nano-Flake/Micro-Flower Iron Fluoride with Hydration Water Induced Tunnels for Secondary Lithium Battery Cathodes. *Nano Energy* **2017**, *32*, 10−18.
(30) Di Carlo, L.; Conte, D. E.; Kemnitz, E.; Pinna, N. Microwave-Assisted Fluorolytic Sol-Gel Route to Iron Fluoride Nanoparticles for Li-Ion Batteries. *Chem. Commun.* **2014**, *50*, 460−462.
(31) Kim, S. W.; Seo, D. H.; Gwon, H.; Kim, J.; Kang, K. Fabrication of FeF_3 Nanoflowers on CNT Branches and Their Application to High Power Lithium Rechargeable Batteries. *Adv. Mater.* **2010**, *22*, 5260−5264.
(32) Li, B.; Zhang, N.; Sun, K. Confined Iron Fluoride@CMK-3 Nanocomposite as an Ultrahigh Rate Capability Cathode for Li-Ion Batteries. *Small* **2014**, *10*, 2039−2046.
(33) Li, C.; Gu, L.; Tsukimoto, S.; van Aken, P. A.; Maier, J. Low-Temperature Ionic-Liquid-Based Synthesis of Nanostructured Iron-Based Fluoride Cathodes for Lithium Batteries. *Adv. Mater.* **2010**, *22*, 3650−3654.
(34) Li, L.; Jacobs, R.; Gao, P.; Gan, L.; Wang, F.; Morgan, D.; Jin, S. Origins of Large Voltage Hysteresis in High-Energy-Density Metal Fluoride Lithium-Ion Battery Conversion Electrodes. *J. Am. Chem. Soc.* **2016**, *138*, 2838−2848.
(35) Li, L.; Meng, F.; Jin, S. High-capacity Lithium-ion Battery Conversion Cathodes Based on Iron Fluoride Nanowires and Insights Into the Conversion Mechanism. *Nano Lett.* **2012**, *12*, 6030−6037.
(36) Liu, J.; Wan, Y.; Liu, W.; Ma, Z.; Ji, S.; Wang, J.; Zhou, Y.; Hodgson, P.; Li, Y. Mild and Cost-Effective Synthesis of Iron Fluoride−Graphene Nanocomposites for High-Rate Li-Ion Battery Cathodes. *J. Mater. Chem. A* **2013**, *1*, 1969−1975.
(37) Ma, D. L.; Cao, Z. Y.; Wang, H. G.; Huang, X. L.; Wang, L. M.; Zhang, X. B. Three-Dimensionally Ordered Macroporous FeF_3 and its in situ Homogenous Polymerization Coating for High Energy and Power Density Lithium Ion Batteries. *Energy Environ. Sci.* **2012**, *5*, 8538−8542.
(38) Ma, R.; Lu, Z.; Wang, C.; Wang, H. E.; Yang, S.; Xi, L.; Chung, J. C. Large-Scale Fabrication of Graphene-Wrapped FeF_3 Nanocrystals as Cathode Materials for Lithium Ion Batteries. *Nanoscale* **2013**, *5*, 6338−6343.
(39) Myung, S. T.; Sakurada, S.; Yashiro, H.; Sun, Y. K. Iron Trifluoride Synthesized via Evaporation Method and Its Application to Rechargeable Lithium Batteries. *J. Power Sources* **2013**, *223*, 1−8.
(40) Shinde, V. V.; Jeong, Y. T. Sonochemical FeF_3 Catalyzed Three-Component Synthesis of Densely Functionalized Tetrahydroindazolo-[3,2-b]Quinazoline Under Solvent-Free Conditions. *Tetrahedron Lett.* **2016**, *57*, 3795−3799.
(41) Tan, H. J.; Smith, H. L.; Kim, L.; Harding, T. K.; Jones, S. C.; Fultz, B. Electrochemical Cycling and Lithium Insertion in Nanostructured FeF_3 Cathodes. *J. Electrochem. Soc.* **2014**, *161*, A445−A449.
(42) Tan, J. L.; Liu, L.; Hu, H.; Yang, Z. H.; Guo, H. P.; Wei, Q. L.; Yi, X.; Yan, Z. C.; Zhou, Q.; Huang, Z. F.; et al. Iron Fluoride with Excellent Cycle Performance Synthesized by Solvothermal Method as Cathodes for Lithium Ion Batteries. *J. Power Sources* **2014**, *251*, 75−84.
(43) Wang, F.; Robert, R.; Chernova, N. A.; Pereira, N.; Omenya, F.; Badway, F.; Hua, X.; Ruotolo, M.; Zhang, R.; Wu, L.; et al. Conversion Reaction Mechanisms in Lithium Ion Batteries: Study of the Binary Metal Fluoride Electrodes. *J. Am. Chem. Soc.* **2011**, *133*, 18828−18836.
(44) Yabuuchi, N.; Sugano, M.; Yamakawa, Y.; Nakai, I.; Sakamoto, K.; Muramatsu, H.; Komaba, S. Effect of Heat-Treatment Process on FeF_3 Nanocomposite Electrodes for Rechargeable Li Batteries. *J. Mater. Chem.* **2011**, *21*, 10035−10041.
(45) Zhao, X.; Hayner, C. M.; Kung, M. C.; Kung, H. H. Photothermal-Assisted Fabrication of Iron Fluoride-Graphene Composite Paper Cathodes for High-Energy Lithium-Ion Batteries. *Chem. Commun.* **2012**, *48*, 9909−9911.

DOI: 10.1021/acs.chemmater.7b04743
Chem. Mater. 2018, 30, 1825−1829